Climatic variations of the work done by the wind on the ocean's general circulation

J. M. Lauderdale,[1,2] A. C. Naveira Garabato,[2] K. I. C. Oliver,[2] and L. N. Thomas[3]

Received 19 April 2012; revised 1 August 2012; accepted 1 August 2012; published 14 September 2012.

[1] The Southern Hemisphere westerlies exert an important influence on global climate, supplying nearly half of the mechanical energy for the deep overturning circulation. In a coarse-resolution ocean model, northward-shifted winds increase the work done on surface geostrophic flows due to enhanced velocities associated with the Antarctic Circumpolar Current (ACC). Alternatively, energy supply is diminished by southward-shifted winds, primarily through reduced correspondence between wind stress and surface velocity in the Southern Ocean due to dynamical and topographic constraints on the ACC. When combined perturbations in latitude and magnitude of the westerlies are applied, these results are reconciled with estimates of recent trends in wind work and volume transport in the Southern Ocean from observations and coupled climate models. This indicates that the strength of the winds exerts a dominant effect that masks the opposing consequences of latitudinal migration. In particular, transport through Drake Passage shows a clear relationship with wind work and velocity when the winds move poleward leading to a reduction in all three quantities. However, under equatorward-shifted winds, stronger polar easterlies adjacent to the Antarctic continent establishes a recirculation gyre leading to increased mechanical energy input and swifter currents but reduced transport. Significant (**O**(25%)) changes in the mechanical energy supply from the winds may be possible on climatic time scales, particularly associated with the spatial correlation between winds and the ACC that does not depend critically on unresolved eddy processes in this model, leading to a pathway for altering abyssal diapycnal mixing rates and stratification of the ocean interior.

Citation: Lauderdale, J. M., A. C. Naveira Garabato, K. I. C. Oliver, and L. N. Thomas (2012), Climatic variations of the work done by the wind on the ocean's general circulation, *J. Geophys. Res.*, *117*, C09017, doi:10.1029/2012JC008135.

1. Introduction

[2] The meridional overturning circulation (MOC) is a largely mechanically driven system that transports significant amounts of heat and freshwater and determines the vertical distribution of carbon and nutrients. Abyssal stratification is maintained by the downward flux of buoyancy associated with turbulent diapycnal mixing [*Munk and Wunsch*, 1998] and wind-driven upwelling [*Toggweiler and Samuels*, 1998; *Webb and Suginohara*, 2001], converting kinetic energy to gravitational potential energy. According to *Munk and Wunsch* [1998], this energy is mainly derived from tidal dissipation (around 1 TW) [*Egbert and Ray*, 2000] and surface winds acting on the ocean's geostrophic circulation (0.76–0.91 TW) [*Wunsch*, 1998; *Hughes and Wilson*, 2008; *Scott and Xu*, 2009]. The work done by the wind is dominated by forcing of the Antarctic Circumpolar Current (ACC) by the Southern Hemisphere Westerly winds. Recent studies have identified that a significant proportion (0.2–0.5 TW) of mechanical energy input is used to generate internal gravity waves where geostrophic flows impinge on rough topography, particularly in the Southern Ocean [*Nikurashin and Ferrari*, 2011; *Scott et al.*, 2011]. Internal wave breaking transfers energy to small-scale turbulence, leading to dissipation and, with roughly 20% efficiency, diapycnal mixing of buoyancy.

[3] Both energy sources have likely undergone significant variations in the past and could respond to future climatic changes. For example, reduced sea level during glacial periods may have produced enhanced tidal flows and dissipation [*Egbert et al.*, 2004; *Green et al.*, 2009]. On the other hand, tidal dissipation depends on uncertain glacial stratification that seemingly increased in the Southern Ocean [*Adkins et al.*, 2002], possibly inhibiting diapycnal mixing [*Watson and Naveira Garabato*, 2006]. On balance, tidal enhancement is thought to have primarily occurred in the North

[1]School of Environmental Sciences, University of Liverpool, Liverpool, UK.
[2]Ocean and Earth Science, National Oceanography Centre, Southampton, University of Southampton, Southampton, UK.
[3]Department of Environmental Earth System Science, Stanford University, Stanford, California, USA.

Corresponding author: J. M. Lauderdale, School of Environmental Science, University of Liverpool, 4 Brownlow St., Liverpool L69 3GP, UK. (j.lauderdale@liverpool.ac.uk)

0148-0227/12/2012JC008135

Atlantic [*Oliver and Edwards*, 2008] with similar or slightly reduced tidal amplitude in the remainder of the abyss compared to present conditions [*Arbic et al.*, 2008].

[4] It has been hypothesized that an equatorward shift or reduction of the Southern Hemisphere Westerlies may have contributed to the glacial-interglacial atmospheric CO_2 cycles by decreasing deep water ventilation [e.g., *Toggweiler et al.*, 2006], which has received some support from paleoceanographic evidence [e.g., *Anderson et al.*, 2009]. Proxy records of $\delta^{18}O$ and $\delta^{13}C$ examined by *Govin et al.* [2009] suggest a northward migration of the Southern Ocean hydrographic fronts and decreased upwelling of deep waters consistent with the paradigm of northward shifted winds during the Last Glacial Maximum (LGM). However, *Matsumoto et al.* [2001] discerned no change in ACC frontal position from their latitudinal $\delta^{18}O$ distributions. Furthermore, a northward migration of fronts might increase deep water outcrop area leading to increased outgassing of CO_2 [*Tschumi et al.*, 2008]. A variety of proxies from Australasia assessed by *Shulmeister et al.* [2004] point to enhanced westerly winds at the LGM and reduced winds at the start of the Holocene. Varied results from coupled climate model simulations for the Paleoclimate Model Intercomparison Project (PMIP) [e.g., *Menviel et al.*, 2008] and general circulation models of the atmosphere or ocean [e.g., *Kitoh et al.*, 2001; *Shin et al.*, 2003; *Otto-Bliesner et al.*, 2006; *Williams and Bryan*, 2006] also suggest that the precise nature of wind anomalies at the LGM remains equivocal.

[5] Conversely, the recent interdecadal positive trend in the Southern Annular Mode (SAM), the dominant pattern of extra-tropical variability in the Southern Hemisphere, is associated with stronger, poleward-shifted winds [*Thompson and Solomon*, 2002] linked to the effects of anthropogenic warming [*Fyfe and Saenko*, 2005]. However, the seasonality and period of these wind stress trends appears to be more consistent with ozone depletion [*Yang et al.*, 2007], while recent studies that investigated the consequences of the recovery of the Antarctic ozone hole in climate-chemistry models found Southern Hemisphere warming and a robust reversal in the SAM trend over the next century [*Perlwitz et al.*, 2008; *Butchart et al.*, 2010; *Polvani et al.*, 2011].

[6] Inferring how changes in the strength and latitude of the Southern Hemisphere Westerly winds will impact the rate at which mechanical energy is imparted to the ocean's general circulation is also far from obvious due to the fundamentally non-zonal nature of the ACC and the dependence of the response to wind forcing on complex dynamics, implicating flow-topography interactions [e.g., *Hughes and de Cuevas*, 2001], mesoscale eddy processes [e.g., *Hallberg and Gnanadesikan*, 2006], buoyancy effects [e.g., *Cai and Baines*, 1996], and sensitivity to winds outside the Drake Passage latitude band [*Allison et al.*, 2010].

[7] In this paper, we conduct a series of idealized wind perturbation experiments with a coarse-resolution ocean model to investigate the mechanisms by which variations in the strength and latitude of the Southern Hemisphere Westerlies might affect the input of mechanical energy to the ocean. The wind fields constructed are informed by observational and model analyses but are not intended to recreate the details of the LGM or a warmer future planet. We find that substantial (**O**(25%)) changes in wind work are possible in an ocean with parameterized eddies, with north-shifted (south-shifted) Southern Ocean winds generally resulting in increased (decreased) wind work except under significant decreases (increases) in wind stress magnitude. We argue that at least some major elements of those changes are likely to carry over to the eddying regime.

2. Model and Methods

[8] A 2.8° × 2.8° global rigid lid configuration of the Massachusetts Institute of Technology general circulation model (MITgcm) [*Marshall et al.*, 1997] is used to investigate the mechanisms of climatic variations of wind work. It has 15 non-uniform vertical levels and is forced by a repeating 12-month cycle of heat and freshwater fluxes [*Jiang et al.*, 1999] with relaxation toward climatological sea surface temperature and salinity over timescales of 60 and 90 days, respectively. The mesoscale eddy field is parameterized using the *Gent and McWilliams* [1990] scheme with an eddy diffusivity of 1×10^3 m^2 s^{-1} and a diapycnal diffusivity of 5×10^{-5} m^2 s^{-1}. Winds for the control run (CNTRL) are provided by *Trenberth et al.* [1989] (Figure 1a). Further details about model configuration and spin-up are given by *Lauderdale* [2010].

[9] The CNTRL steady state is perturbed by shifting the zonal wind stress peak three grid-points (nominally 10°, as suggested by *Toggweiler et al.*'s [2006] scrutiny of available paleoceanographic data) north (N10DEG) or south (S10DEG) whilst maintaining in situ wind stress magnitude (Figure 1a) and run until the model no longer drifts (∼5000 years, but the majority of the adjustment occurs in the first millennium). Secondly, from the initial state, the magnitude of the shifted winds are scaled so that the global integral of the zonal wind stress remains equal to that of the control (N10GEO and S10GEO), thus taking into account the geometric effect of the different grid size (or longitudinal integration length) over which the westerlies are located. Integrating the stronger winds used in S10GEO around a smaller latitude band (∼4500 km shorter than CNTRL) returns the same value as integrating the weaker winds used in N10GEO around a longer latitude band (∼3500 km longer than CNTRL). Differences in wind work are thus due to changes in ocean circulation or in the juxtaposition between the intense winds and currents.

[10] Coupled models forced by changes in greenhouse gas concentrations [e.g., *Saenko et al.*, 2005; *Russell et al.*, 2006a, 2006b] and 25 years of observations of the Southern Ocean winds [e.g., *Huang et al.*, 2006, and references therein] suggest a composite change in the westerlies, with a modest southward migration (∼3°) and an intensification of **O**(50%). To investigate the effect of these superimposed anomalies, two further sets of experiments are considered. A third set of wind fields, N03DEG and S03DEG, are constructed along the same lines as the N/S10DEG by maintaining the CNTRL peak wind stress in the Southern Ocean, but this time the latitudinal shift is limited to one grid point (nominally 3°). Finally, in accord with recent observations and glacial-interglacial hypotheses, the magnitude of the wind field from S03DEG is increased by 50% (S03STRONG) while the magnitude of the wind field from N03DEG is decreased by 50% (N03WEAK). A summary of the different wind stress forcing fields is given in Table 1.

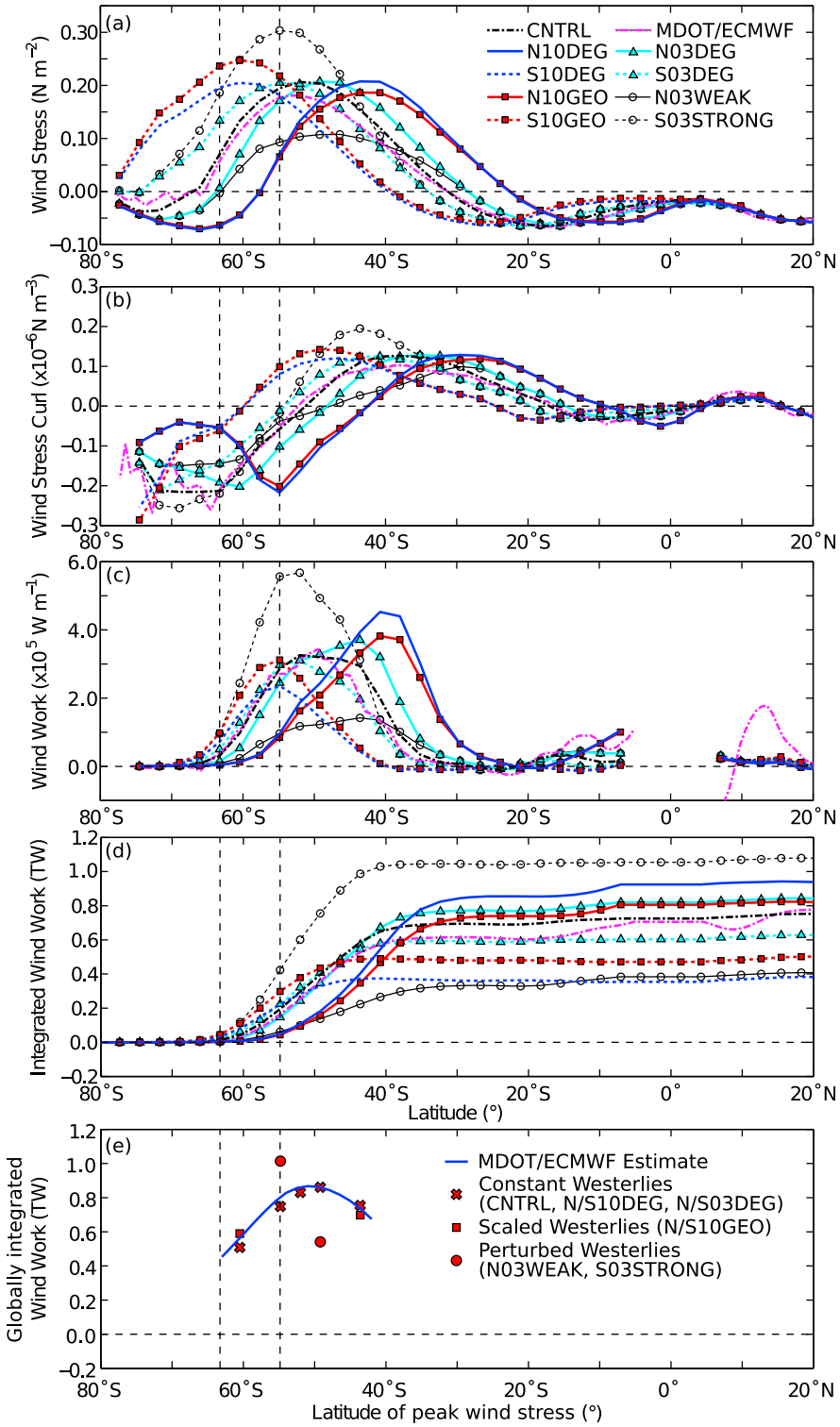

Figure 1. Profiles of (a) zonal-mean wind stress, (b) zonal-mean wind stress curl, (c) zonally-integrated wind work and (d) south to north cumulatively integrated wind work. North-shifted winds have solid lines and south-shifted winds have dotted lines, see the key, text and Table 1 for details. The MDOT/ECMWF fields are estimated from observations using *Maximenko et al.* [2009] mean dynamic topography (MDOT) and ECMWF interim wind stresses [*Dee et al.*, 2011]. All the profiles north of 20°N are equal and unperturbed. (e) The globally integrated wind work resulting from shifting the peak westerly winds over a constant surface geostrophic velocity field (W_τ) for the MDOT/ECMWF fields (solid line) and control geostrophic velocity and perturbed winds stress fields from Figure 1a for the model estimate (symbols). The location of Drake Passage (~55–63°) is indicated by vertical dashed lines.

Table 1. Summary of the Details of the Wind Perturbation Experiments Described in Section 2 and Figure 1[a]

Experiment	Peak τ_x (Nm^{-2})	Latitude (deg)
CNTRL	0.206	−52.0
N10DEG	0.207	−43.6
S10DEG	0.205	−60.5
N10GEO	0.186	−43.6
S10GEO	0.247	−60.5
N03DEG	0.207	−49.2
S03DEG	0.205	−54.8
N03WEAK	0.107	−49.2
S03STRONG	0.303	−54.8

[a]Peak τ_x is the Southern Ocean maximum of zonal-average westerly wind stress while Latitude is the latitude at which this maximum occurs.

[11] Globally integrated wind work (W) is diagnosed from equation (1), comprising wind stress forcing, τ, and large-scale surface geostrophic circulation, $\mathbf{v}_g$, calculated from sea surface height anomaly, integrated over surface area, A,

$$W = \int (\tau \cdot \mathbf{v}_g) dA. \quad (1)$$

A region of ±4° about the equator is excluded from the geostrophic calculations due to a singularity related to the Coriolis parameter and also because the equatorial region hosts a differing dynamical regime where equation (1) is invalid [*Wunsch*, 1998].

[12] The surface geostrophic velocity field from CNTRL is verified by comparison with surface height anomaly from the steady state circulation and the mean dynamic ocean topography (MDOT) of *Maximenko et al.* [2009]. The model corresponds well with the observations, capturing the large scale patterns of the subtropical gyres and the Northern Hemisphere subpolar gyres ($R^2 = 0.96$). Furthermore, the location and gradient of the climatological sea surface slope across the ACC in the Southern Ocean agree in both the global zonal average and in the South Atlantic in particular ($R^2 = 0.95$), with perhaps a ∼1° northward bias in the model sea surface slope. However the model's coarse resolution results in a poor representation of the equatorial current system and the shedding of Agulhas rings in the South Atlantic, which leads to dissimilarities between the two dynamic height profiles in the subtropical gyre to the north of 40°S. Nevertheless, the surface height anomaly from this coarse resolution model appears to be providing an adequate representation of the surface geostrophic circulation. Volume transport through Drake Passage in CNTRL is 139.8 Sv (1 Sv ≡ 10^6 m^3 s^{-1}), which lies within the range of observational [e.g., *Cunningham et al.*, 2003] and inverse model [e.g., *Ganachaud and Wunsch*, 2000] estimates.

[13] Finally, to support the inferences of the model perturbations we derive an observational estimate of the mechanical energy flux using MDOT to obtain geostrophic surface velocities and mean monthly European Centre for Medium Range Weather Forecasting (ECMWF) interim wind stress fields [*Dee et al.*, 2011], using all the available data until the end of 2011. The zonal wind stress is slightly weaker than used in the model (Figure 1a) and the peak is shifted slightly to the south, however the wind stress curl is very similar between the two fields (Figure 1b). The derived geostrophic velocities were averaged onto the coarser 0.75 × 0.75° ECMWF grid, the stresses were averaged in time and, in keeping with the treatment of the model data, ±4° about the equator was excluded.

3. Model Response to Perturbed Southern Hemisphere Winds

[14] In this section, we detail the response of the the Southern Ocean to perturbed winds, describing the circulation changes and then the changes in mechanical energy fluxes associated with wind work before investigating the mechanisms behind these anomalies and lastly the implications of these changes on the global ocean.

3.1. Changes in Southern Ocean Circulation

[15] Forced by shifted winds (Figure 1a), the modeled ACC migrates latitudinally. The control position of the maximum in mean zonal geostrophic velocity is located at 47°S. For N10DEG, this maximum is increased and located ∼6° further north at 41°S, while it is shifted southward to 55° in S10DEG and reduced in magnitude. This pattern of a shifting ACC is repeated for the remaining experiments with changes in magnitude of the winds resulting in increases or decreases in ACC velocity. The mean location of the circumpolar current generally corresponds with the latitudes of maximum zonal-mean wind stress, zero zonal-mean wind stress curl and maximum zonally-integrated wind work in Figures 1a–1c, which also holds for the observational data. However, this relationship appears to break down for the larger shifts used in S10DEG and S10GEO, where the positions of maximum zonal-mean wind stress and zero zonal-mean wind stress curl lie further south at roughly 60°S (near the centre of Drake Passage) compared to the position of peak zonal velocity and maximum zonally-integrated wind work at 55°S.

[16] Volume transport through Drake Passage (TDP), which is often used to compare observations of the ACC and models, also reveals an interesting relationship with Southern Hemisphere winds (Table 2). When winds are shifted poleward in experiments S10DEG, S10GEO and S03DEG, Drake Passage transport decreases as anticipated from reduced geostrophic velocity. However, ACC transport through this choke point is also reduced under the equatorward-shifted winds in N10DEG, N10GEO and N03DEG, despite swifter geostrophic ACC velocities. This situation is illustrated in Figures 2a–2c for the N10DEG, CNTRL and S10DEG experiments. For the northward-shifted winds, the expanded region of polar easterlies adjacent to the Antarctic continent and increasingly positive wind stress curl (Figure 1b) establishes a ∼20 Sv gyre that allows ACC velocities, particularly in the Atlantic and Indian Oceans, to remain vigorous while supporting reduced volume transport through Drake Passage. The relationship between ACC velocity and volume transport through Drake Passage is recoupled when the ocean is forced by large perturbations in the strength of the shifted Southern Hemisphere westerlies (Figures 2d and 2e): compared to CNTRL, N03WEAK has slower geostrophic velocities and reduced transport through Drake Passage, whereas S03STRONG has faster geostrophic velocities and larger Drake Passage transport, in agreement with the results of coupled climate models [e.g., *Russell et al.*, 2006a, 2006b; *Sen Gupta and England*, 2006].

[17] The north- or southward displacement of the ACC is also echoed in expansion and contraction of the subtropical gyres, where the gyre boundary is defined as the zonally

Table 2. Resulting Model Diagnostics Due to Latitudinal Shifts in the Westerly Winds[a]

Experiment	TDP (Sv)	Latitude ($\psi^{baro} = 0$) (°S)	W (TW)	W_{SO} (TW)	W_{gyre} (TW)	W_{τ} (TW)	W_0 (TW)	$\int\|\mathbf{v_g}\|dA$ (10^{13} N)	$\int\|\tau\|dA$ (10^{13} m^3 s^{-1})	W/W_0
CNTRL	139.8	41.6	0.83	0.65	0.18	0.83	0.80	2.311	0.894	1.04
N10DEG	99.8	36.6	1.01	0.77	0.24	0.75	1.00	2.462	1.049	1.02
S10DEG	110.4	46.4	0.46	0.36	0.10	0.51	0.62	2.102	0.767	0.74
N10GEO	92.2	40.1	0.90	0.66	0.23	0.70	0.92	2.343	1.018	0.98
S10GEO	127.9	43.6	0.58	0.47	0.11	0.59	0.67	2.229	0.779	0.87
N03DEG	137.2	40.1	0.92	0.67	0.25	0.86	0.87	2.361	0.953	1.06
S03DEG	136.3	43.6	0.71	0.55	0.16	0.75	0.74	2.270	0.849	0.95
N03WEAK	83.3	40.1	0.49	0.27	0.22	0.54	0.62	1.860	0.859	0.79
S03STRONG	187.0	43.6	1.16	0.99	0.17	1.01	0.97	2.735	0.917	1.20

[a]TDP is the ACC transport through Drake Passage and Latitude ($\psi^{baro} = 0$) is the zonal average latitude of the zero barotropic transport as a proxy for the boundary between the Southern Ocean and the subtropical gyres (Figure 2). W is the globally integrated wind work from (1), while W_{SO} and W_{gyre} are integrated wind work to the south and north of that latitude, respectively. W_{τ} is the wind work calculated using the control geostrophic circulation and perturbed wind field (symbols in Figure 1e). W_0 is the characteristic wind work scale (2) obtained from the area-weighted product of the integrated magnitudes of the wind stress ($\int|\tau|dA$) and surface geostrophic speed ($\int|\mathbf{v_g}|dA$), using a surface area of 2.595×10^{14} m^2. W/W_0 is a metric of the spatial correlation between wind stress and surface velocity calculated by normalizing wind work by the wind work scale.

averaged latitude of zero barotropic transport, which separates the eastward ACC flow from the eastward flow associated with the subtropical gyres (Figure 2 and Table 2). Furthermore, the volume transport of the subtropical gyres is increased or decreased ~10–20 Sv in response to altered latitude of peak westerly wind stress and changes in wind stress curl, although it is possible that the modest values for this in the model may depend on the relaxing surface buoyancy boundary conditions, which might restrict gyre movement.

3.2. Change in Mechanical Energy Input due to Perturbed Southern Hemisphere Westerlies

[18] The globally integrated work done by the wind in CNTRL is 0.83 TW. The overall magnitude and distribution

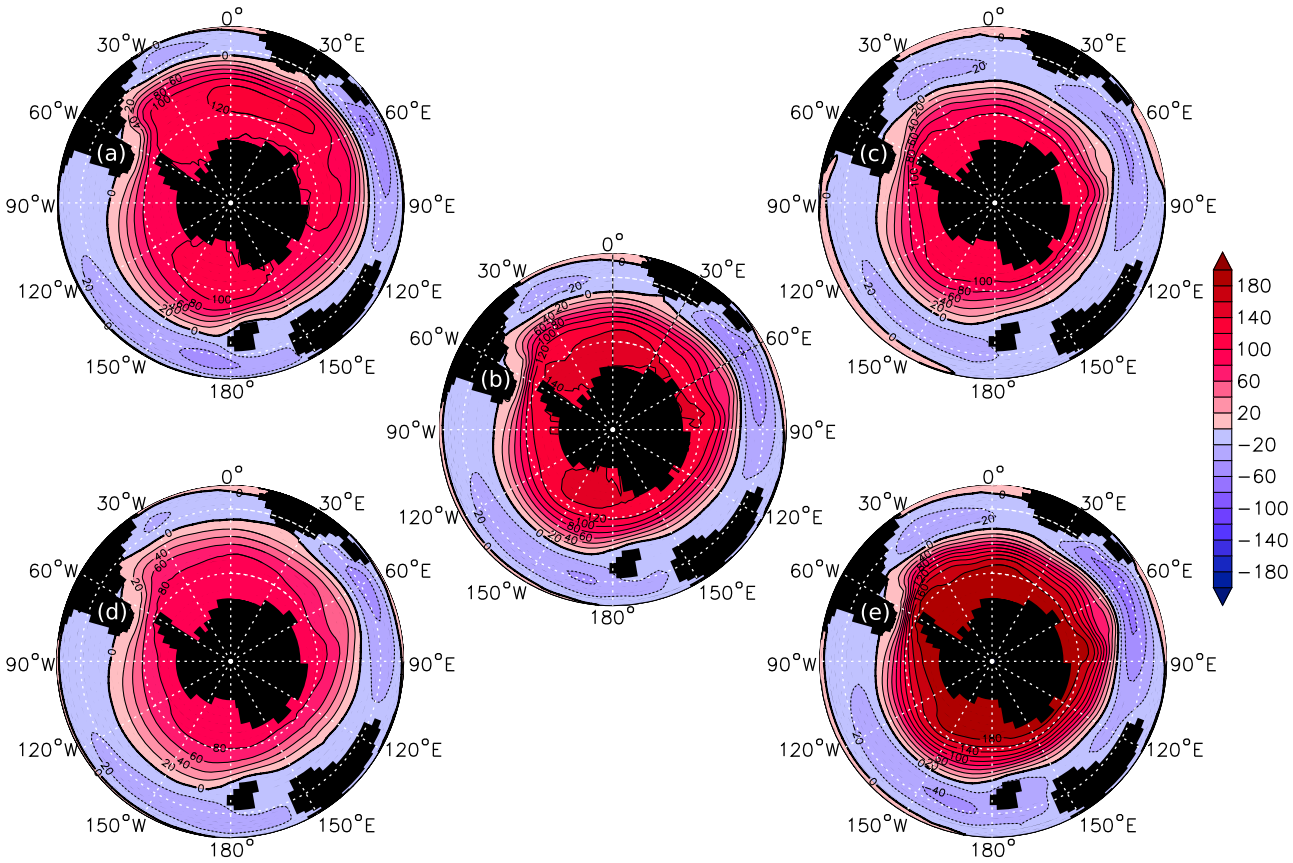

Figure 2. Surface barotropic stream function in the Southern Hemisphere (Sv) for (a) N10DEG, (b) CNTRL, (c) S10DEG, (d) N03WEAK and (e) S03STRONG. Latitude circles from equator to pole are at 0°, 30°S and 60°S.

of wind work in CNTRL compares well to the global estimate derived from MDOT and ECMWF data, which yields 0.86 TW of globally integrated wind work. While the observed peak wind work is a similar magnitude, the model peak extends further to the north, probably as a result of the models coarse resolution spreading out the ACC. Just over three-quarters of wind work (0.64 TW) is input south of 40°S in the model while the equivalent value for the observations is 0.58 TW. The remainder is accounted for by more dynamic and better resolved equatorial current system (Figure 1d).

[19] Both calculations probably overestimate the mechanical energy flux by neglecting the effect of mesoscale eddies due to the relatively coarse-resolution of the MDOT/ECMWF data as well as the coarse-resolution model, although this is considered fairly small (±10's GW) [e.g., *Hughes and Wilson*, 2008; *Scott and Xu*, 2009], and not accounting for surface currents in the shear from which wind stress is derived [*Duhaut and Straub*, 2006; *Hughes and Wilson*, 2008; *Hutchinson et al.*, 2010] leading to a larger ∼30%, or approximately 0.2 TW, enhancement.

[20] Interestingly, only one-quarter of globally integrated wind work from both sources is imparted at the latitude of Drake Passage (55–63°) as the ACC generally lies to the north of this location. Boundary currents such as the Kuroshio and Gulf Stream gain mechanical energy from the winds, whilst the subtropical regions host negligible or occasionally slightly negative wind work.

[21] The mechanical energy flux by the winds is increased to 1.01 TW in N10DEG (see also Table 2). Figures 1c and 1d show a greater amount of work is done in N10DEG on the Southern Ocean's geostrophic circulation compared to CNTRL, providing the northward migration of the ACC is taken into account. If the boundary between the Southern Ocean to the south and gyres to the north is taken to be the zonally-average latitude of zero transport in the surface barotropic stream function then wind work accumulates to 0.77 TW poleward of 36.6° in N10DEG compared to 0.65 TW south of 41.6°in CNTRL. Note that we do not expect this latitude to be the same as the latitude of zero wind stress curl, which determines the mean latitude of the ACC as described above. Less wind work is done in the latitudes of Drake Passage in N10DEG compared to CNTRL because of the northward migration of the ACC and the westerlies. In contrast, the rate of wind work decreases in S10DEG to 0.46 TW due to a significant decline in wind work in the Southern Ocean region to 0.36 TW. Considering just the mechanical energy input into the ocean by the wind in the unblocked latitudes of Drake Passage, more wind energy is imparted there in S10DEG than for CNTRL or N10DEG (Figures 1c and 1d) but as just described, the order is reversed when considering the global integral.

3.3. Determining the Causes for Wind Work Anomalies

[22] Mechanical energy input by the wind may be altered by variations in the magnitude of the wind stress, changes in surface geostrophic velocity, or the spatial correlation between the two. In this section, we attempt to tease apart these effects.

[23] Adjusting the strength of the westerly winds to take into account the length of integration for the wind stress and maintain the CNTRL integral of τ_x damps the anomalies in wind work described for N/S10DEG, producing wind work values of 0.90 TW and 0.58 TW for N10GEO and S10GEO, respectively. These experiments suggest that about half of the wind work anomalies seen in N10DEG and S10DEG may be associated with the winds and ocean currents with half attributed to the geometric effect of latitude circle on the strength of integrated wind work. The perturbations with more modest shifts in the Southern Ocean winds show a similar tendency in integrated wind work as the large shifts, with the rate of wind work increasing to 0.92TW in N03DEG and decreasing to 0.71 TW in S03DEG compared to CNTRL. Although there is a slight geometric effect associated with these anomalies, it is estimated at approximately 0.03 TW, or a quarter of the difference between N/S10DEG and N/S10GEO (due to a 1000 km difference in latitude circle for a 3° shift compared to 4000 km on average for a ∼10° shift). However, when both the latitude and the magnitude of the westerlies are perturbed then integrated wind work increases to 1.16 TW in S03STRONG and decreases to 0.49 TW in N03WEAK. Clearly, the initial change in work done by the wind caused by the shift in latitude in N/S03DEG is swamped by the much greater effect of the 50% change in magnitude in N03WEAK and S03STRONG.

[24] Changes in the location and strength of the subtropical gyres only marginally affects the rate of mechanical energy input. Using the partition of globally integrated wind work into "Southern Ocean", W_{SO}, and "northern gyre", W_{gyre}, components in Table 2, the majority of the changes in W appear in the Southern Ocean region directly associated with the ACC and the westerlies, coupled to the migration of the gyre boundary. There is some effect of spin-up or spin-down of the northern gyres on the integrated wind work anomaly of less than ∼0.1 TW compared to CNTRL. Again, the modest values here may depend on the relaxing surface buoyancy boundary conditions.

[25] By assuming that the ACC does not respond to the migrating latitude of the peak Southern Hemisphere winds, an estimate of wind work can be calculated that depends only on the correlation between the westerlies, the "fixed" ACC and constant Southern Ocean/northern gyre boundary (W_τ in Table 2). For the MDOT/ECMWF data, the geostrophic velocity and Northern Hemisphere wind field was held constant while the zonal wind stress peak in the Southern Hemisphere was migrated between 42–63°S. For the model experiments, wind work was calculated using the nine different wind stress fields and the geostrophic circulation of CNTRL. The majority of the wind stress perturbations in our model agree with the MDOT/ECMWF values that show simply moving the latitude of peak westerlies results in a small decline in W for equatorward shifts and a larger reduction in W for poleward shifts (Figure 1e). Furthermore, the observational curve peaks at its original position (or a shift of zero degrees) confirming that the ACC and Southern Hemisphere westerlies are well aligned to the north of Drake Passage in nature, as in the model. Only N03WEAK and S03STRONG, where the westerlies have had a significant magnitude change of 50%, lie away from the MDOT/ECMWF line, where the peak wind stress has the same average magnitude. Again, this demonstrates that the change in work done by migration of the winds can be overshadowed by the opposing effects of changing their magnitude.

[26] Now, comparing the model values of W with the values of W_τ under different forcing scenarios (Table 2)

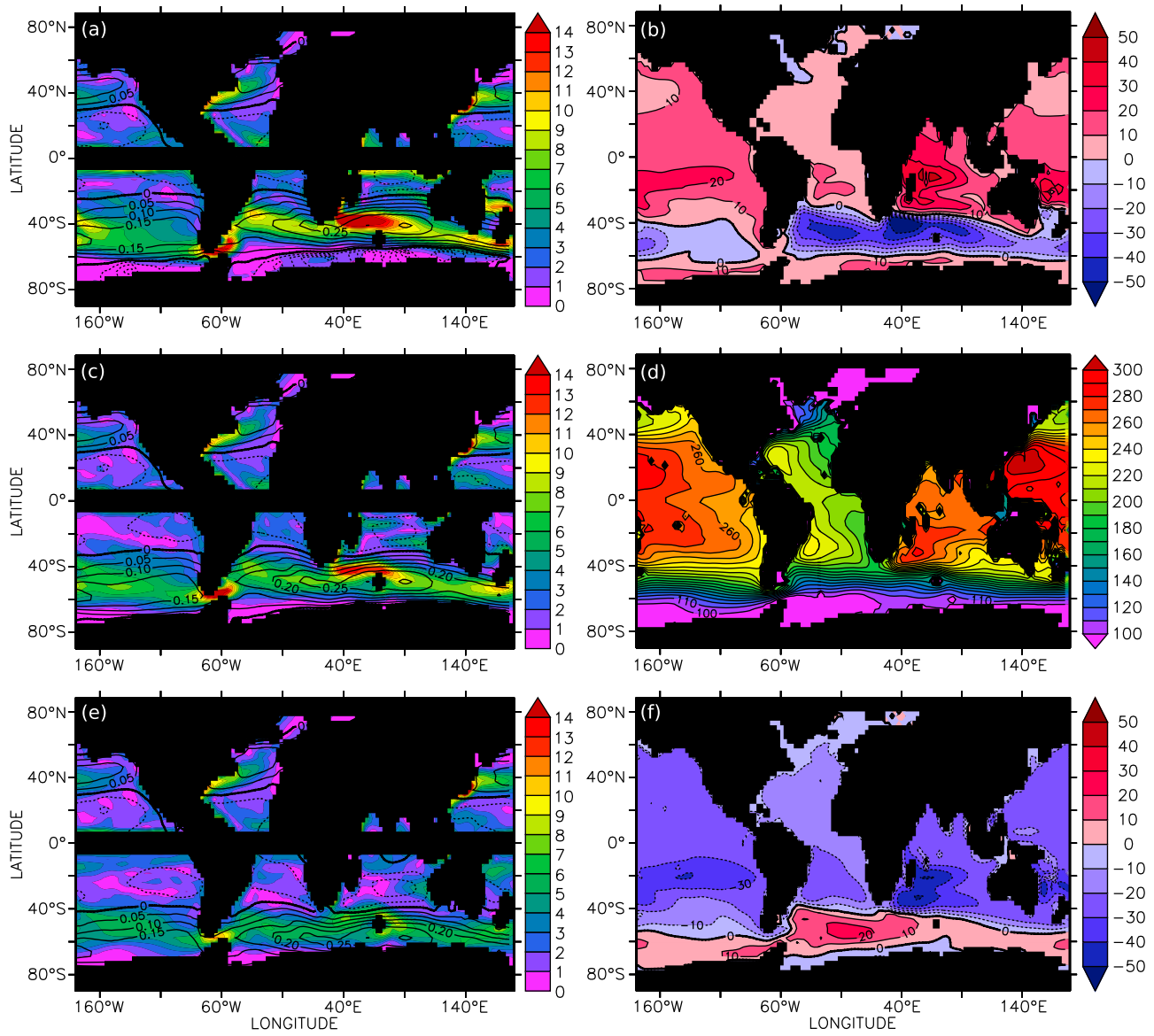

Figure 3. Surface geostrophic speed (cm s^{-1}) overlaid with contours of zonal wind stress (N m^{-2}) for (a) N10DEG, (c) CNTRL and (e) S10DEG. (d) Vertically integrated steric height between 0–2 km for CNTRL (dyn-cm) and vertically integrated steric height anomalies (dyn-cm) over the same depth range for (b) N10DEG and (f) S10DEG.

reveals a fairly large difference for northward shifts of the westerlies but considerably smaller differences between W and W_τ when the winds are shifted to the south. This suggests that the decreases in wind work when the westerlies are shifted poleward is largely due to reduced correspondence of the locations of strong winds and ocean currents, with a modest deceleration of the ACC necessary to reduce W_τ to W in S10DEG and S03DEG while the ACC shifts as far south as it is able. Whereas, the increased wind work when the westerlies are shifted to the north obviously relies on the migration of the ACC and increased velocities to supply the extra ~0.2 TW to increase W_τ to W in N10DEG and N10GEO and to a lesser degree for N03DEG. Similarly, N03WEAK requires the ACC to respond to the 50% weaker winds with reduced velocities while S03STRONG suggests acceleration of the ACC.

[27] Superimposing maps of the magnitude of $\mathbf{v}_g$ and τ_x demonstrates that their degree of correspondence is high in N10DEG (Figure 3a) and CNTRL (Figure 3c). Increased surface geostrophic speed in N10DEG can be seen in the Southern Ocean particularly in the Indian and the Atlantic sectors, where the ACC shows a stronger northward deflection east of Drake Passage compared to CNTRL. Indeed, the extent of co-location between the maximum in surface currents and zonal wind stress to the north of the Kerguelen Plateau is greater for N10DEG than CNTRL, however this is offset by a reduction elsewhere, for example south of the Campbell Plateau or Cape Horn where the ACC is steered around topographic obstructions, away from the peak wind stress. In comparison, S10DEG (Figure 3e) shows a decrease in the magnitude of geostrophic velocity and marked

southward migration of the ACC, with weaker deflection downstream of Drake Passage. However, the ACC still appears to favor the path to the north of the Kerguelen Plateau as in CNTRL, instead of aligning with the peak in wind stress or zero wind stress curl that might suggest passing the obstacle on its southern side. Indeed, the ACC maintains a close association with Australia and New Zealand whereas the wind stress forcing might suggest an increased separation, with the ACC located further poleward. A similar situation also occurs in the Pacific where the ACC remains between the latitudes of 40–60°S, to the north of the Pacific Antarctic Ridge, despite the greater wind stress to the south. This preferred route greatly decreases the association between surface velocity and westerly wind stress, resulting in an overall decrease in wind work.

[28] The compensatory effect of magnitude and correlation of in situ winds and surface currents can be separated numerically by defining a characteristic wind work scale, W_0, obtained from the product of the area-weighted integrated magnitudes of the wind stress and surface geostrophic velocity (equation (2)). W_0 exclusively reflects changes in magnitude of winds and ocean currents because their interactions (contained within the local product of $\mathbf{v}_g$ and τ) are not considered until after the global integration has occurred

$$W_0 = \frac{\int |\tau| dA \cdot \int |\mathbf{v_g}| dA}{\int dA}. \quad (2)$$

The effect of correlation between the wind and velocity fields may then be evaluated by normalizing the calculated value of W by W_0 producing a term that is greater than unity where close association of the westerly winds and the ACC enhances wind work and less than unity where poor correspondence between atmospheric and oceanic currents reduces wind work.

[29] The value of W_0 increases from 0.80 TW for CNTRL to 1.00 TW for N10DEG but decreases to 0.62 TW for S10DEG (Table 2). Considering W_0 alone indicates significant changes in wind work, influenced by altered geostrophic circulation due to altered surface grid area of the wind stress integration, altered distribution of wind stress curl and change in f with latitude. However, normalized wind work that considers the juxtaposition of the winds and the ACC reveals a negligible change from 1.04 for CNTRL to 1.02 for N10DEG and a larger decline to 0.74 for S10DEG as inferred from Figure 3.

[30] The adjusted winds in N10GEO and S10GEO alter the values of both parameters. The changes in W_0 are due to moderate wind stress and velocity anomalies in the Southern Ocean with slightly reduced winds forcing a weaker ACC in N10GEO and slightly stronger winds forcing a more vigorous ACC in S10GEO. Although the path of the ACC in both experiments remains largely unchanged from their unscaled counterparts N/S10DEG, some changes to the spatial correlation between $\mathbf{v}_g$ and τ occur due to greater or reduced convolution in the periphery regions of the wind stress and geostrophic velocity peaks. This response is qualitatively similar in N03DEG and S03DEG but further subdued due to the reduced latitudinal shift. Slightly increased magnitudes and greater correlation between wind stress and surface velocity for N03DEG results in increased integrated wind work. Whereas, in S03DEG, the southward shifted wind decreases both the scale and correlation terms resulting in slightly reduced wind work.

[31] Finally, the compound perturbations in N03WEAK and S03STRONG reverse the pattern seen for the previous experiments. The strong winds and enhanced ACC velocities in S03STRONG increases W_0 compared to CNTRL but the correlation term also increases due to broader agreement between the strong winds and vigorous geostrophic flow in the eastern portion of the Southern Ocean in particular. The sluggish surface currents and winds in N03WEAK result in decreased W_0 while the correlation decreases because the variations in ACC velocity in the different sectors of the Southern Ocean are driven by winds that have a relatively consistent magnitude across the entire region.

3.4. Implications of Altered Mechanical Energy Input by the Winds

[32] The variations in wind work and circulation amongst the different experiments ultimately result in changes in vertically integrated steric height in the upper 2 km throughout the global ocean. The mechanism by which this occurs may be illustrated by considering how changes in the latitudes of Ekman pumping affect the configuration of isopycnals in the ocean interior. Compared to CNTRL, a northward shift in the latitude and an increased magnitude of Ekman pumping deepens isopycnals outcropping to the north of the peak Southern Hemisphere winds and shoals denser isopycnals outcropping south of that maximum [*Luyten et al.*, 1983]. This leads to a general increase in steric height north of ~40°S (Figure 3b) and to a decrease in stratification of the upper ocean, with a reduction in steric height in the ACC region due to the northward migration and tilting of outcropping isopycnals. A southward shift of the winds and associated latitudes of Ekman downwelling causes the low-latitude pycnocline to shoal, resulting in a decrease in steric height (Figure 3f) and an enhancement of stratification in the upper ocean. The ACC region contracts in size relative to N10DEG and exhibits the opposite-sign change due to southward migration and reduced slope of isopycnals.

[33] The relationship between ACC velocity and volume transport through Drake Passage is reiterated by the decoupling of transport and wind work when the westerlies are shifted towards the equator, with northward-shifted winds producing enhanced ACC velocities, increased wind work and reduced transport through Drake Passage. It is the local velocities that determine mechanical energy input, rather than the more integrated diagnostic of volume transport through Drake Passage, which is modified in this instance by the enhanced cyclonic gyre adjacent to Antarctica. Integrated wind work is minimally affected due to the small surface area south of 60°S, although alignment between the easterly winds and the westward currents associated with the southern limb of the gyre lead to slightly elevated wind work in this region, as suggested by the non-symmetric shape of the solid wind work curves in Figure 1c.

[34] Again, when subjected to large perturbations in the magnitude of the shifted Southern Hemisphere Westerlies, the relationship between ACC velocity, volume transport and wind work becomes recoupled with slower geostrophic velocities, reduced Drake Passage transport and decreased

wind work in N03WEAK and faster geostrophic velocities, larger transport through Drake Passage and increased wind work in S03STRONG.

4. Discussion and Conclusions

[35] We have shown that large changes in wind work can result from meridional shifts in the Southern Hemisphere Westerly winds in our model. These changes arise from two distinct factors. The first concerns wind-induced variations in geostrophic velocity. As found by preceding studies [e.g. *Allison et al.*, 2010], the strength of the ACC in ocean models with parameterized eddies is relatively insensitive to wind stress changes in the Drake Passage latitude band and far more sensitive to wind stress changes along the ACC's primary pathway, which lies largely to the north of Drake Passage due to dynamic and topographic constraints (discussed below). This is one of the reasons why experiments such as S10DEG, in which the westerlies overlap extensively with Drake Passage latitudes (Figure 1a), are characterized by reduced ACC velocities and low rates of wind work, whereas experiments such as N10DEG in which the westerlies overlap more closely with ACC streamlines, often to the north of Drake Passage, yield higher ACC velocities and greater wind work values.

[36] The distinction between local ACC velocity and volume transport through the choke point at Drake Passage should be emphasized because, although they change in concert for the poleward-shifted winds in S10DEG, S10GEO and S03DEG, these quantities become decoupled under northward-shifted winds due to the establishment of a recirculation gyre adjacent the Antarctic continent. Compared to CNTRL, this recirculation simultaneously allows vigorous ACC velocities but reduced Drake Passage volume transports in N10DEG, N10GEO and N03DEG. When large changes in magnitude are applied in N03WEAK and S03STRONG then velocity and volume transport become recoupled, with the differences between the S03DEG and S03STRONG experiments reconciling the dichotomy of reduced ACC transports with south-shifted winds in this study (such as S03DEG) compared to greater transports under positive Southern Annular Mode anomalies in coupled climate models [e.g., *Russell et al.*, 2006a, 2006b; *Sen Gupta and England*, 2006]. Large increases in the vigour of the westerlies in these models may be masking the decreases in transport through Drake Passage created by a southward shift alone.

[37] The second factor in determining wind work is the degree of spatial correlation between the winds and the surface geostrophic velocity of the ACC, putting aside the impact of the wind forcing on ACC strength mentioned above. When the winds are shifted to the north, the ACC appears to align with the position of maximum zonal-mean wind stress or zero wind stress curl, generally leading to a good correlation value ($W/W_0 \geq 1$) and increased wind work that peaks at the same latitude. When the winds are shifted to the south by a limited distance (S03DEG and S03STRONG), the ACC responds in a similar way, again aligning with the latitude of zero wind stress curl (also noted by *Oke and England* [2004] and *Saenko et al.* [2005]), resulting in the wind work peak at that location. However, for the larger shifts in S10DEG and S10GEO, this is not the case. The wind stress curl, which is zero at 60°S, would suggest the peaks in current velocity and wind work to be located at the centre of Drake Passage. Instead, they are found at ~55°S, which decreases the correspondence between the atmospheric and oceanic flows ($W/W_0 < 1$) and reduces the efficiency of mechanical energy input from the winds to the oceanic geostrophic circulation.

[38] *Hughes and de Cuevas* [2001] suggest that the north-south meandering path of the ACC is determined by the distribution of bottom pressure torque that balances the wind stress curl, leading to the current being steered around topographic features. The integral of bottom pressure torque across a topographic obstacle gives the form stress that ultimately balances momentum input at the surface by the wind [*Munk and Palmén*, 1951]. Thus, the largely negative wind stress curl associated with the winds in the Southern Ocean is balanced by positive bottom pressure torque, leading to northward deflections of the current over sloping topography. To the north, largely positive wind stress curl is balanced by negative bottom pressure torque, which leads to southward deflections of the ACC around bathymetric features [*Hughes and de Cuevas*, 2001; *Olbers et al.*, 2004]. *Gnanadesikan and Hallberg* [2000] also find that wind stress curl and form stress determine the meridional flow but do not predict zonal flow, which is determined by the large-scale north-south pressure gradient. An investigation into these fundamental dynamics by *Jackson et al.* [2006] examined the response of a circumpolar jet in a wind-forced channel model with idealized topography, including a meridional topographic barrier with a Drake Passage-like gap. They showed that negative bottom pressure torque to the north of a circumpolar jet balanced positive wind stress curl in the subtropical gyre's western boundary current, while negative wind stress curl south of the jet was balanced by positive bottom pressure torque, deflecting the jet northward through a topographic gap. An increase in wind stress magnitude in their model resulted in larger positive bottom pressure torque, increased topographic steering and a more pronounced northward deflection of the jet to balance the wind stress curl.

[39] Our model shows a similar response, with the ACC aligning roughly with the location of zero wind stress curl for north-shifted winds and for limited southward shifts, ultimately guided by bottom pressure torque as suggested by *Hughes and de Cuevas* [2001]. Greater negative wind stress curl in the Southern Ocean in N10DEG, N10GEO and N03DEG also drives a more pronounced northward deflected current after passing through Drake Passage. Again, the S10DEG and S10GEO experiments deviate from this pattern since the location of the peaks in zonal velocity and wind work are further north than the location of maximum wind stress and zero wind stress curl. This illustrates the intimate relationship between the ACC and bottom topography, because if the ACC were to flow zonally south of Cape Horn, the Kerguelen Plateau and further poleward from Australia and New Zealand, topographic obstacles suitable to support form stress would be scarce. For this reason, the ACC is still deflected northward at Drake Passage and the Kerguelen Plateau, albeit less prominently, and hugs the southern Australian coast so as to maintain dynamic balance.

[40] Indeed, this hypothesis is supported by our dual analysis of wind work using a fixed surface geostrophic circulation with perturbed wind stress derived from observed ECMWF/MDOT data and model fields. Mechanical energy input shows a large decline when the winds are shifted to the

south in both model and data. Yet these values using fixed geostrophic circulation are quite close to those obtained from the model when the circulation is allowed to evolve in response to wind forcing. Meanwhile, in order to reconcile the smaller decrease in wind work when the winds are shifted north with fixed geostrophic circulation and the increase in wind work with freely evolving surface circulation, demands that the ACC accelerates and migrates north, consistent with our dynamical arguments above. In summary, dynamics and topographic geometry conspire to constrain the ACC to a relatively invariable path through the Southern Ocean such that the spatial correlation between the westerlies and the ACC is greatest when the winds are displaced northward and vice versa, although the latitude of the circumpolar current appears to be somewhat reactive to a moderate southward displacement of the winds.

[41] Two other studies in particular have looked at changes in wind work under southward shifted Southern Ocean winds: firstly, *Saenko et al.* [2005] simulated a small southward shift of ∼3° and a ∼25% increase in magnitude of the Southern Hemisphere Westerly winds in a coupled model under quadruple CO_2 conditions resulting in a global increase of wind work of a third (rising to nearly one half south of 30°S). Secondly, *Huang et al.* [2006] evaluated a 12% increase in global wind work from altimeter data and from a numerical model forced by a slight southward shift and ∼50% increase in magnitude of the westerlies observed over the last 25 years. One of the features of this study is that the effects of changing the latitude of peak wind stress and its magnitude are considered separately by comparing the S03DEG and S03STRONG experiments. Indeed, for a limited southward shift alone, wind work decreases 15% compared to the control. However, when the combined effects of a modest shift and significant change in magnitude are considered then wind work increased by 40% indicating that the changing strength of the westerlies exerts a dominant effect that masks the opposing results of latitudinal wind migration.

[42] Implications of the mechanical energy budget for the climate was examined by *Gnanadesikan et al.* [2005], who determined that not only was mechanical energy input by the wind in their models of sufficient magnitude to drive vertical and horizontal advection of heat by balancing convection and cabelling (∼0.6 TW), but that wind work was the prime candidate for the source of this energy. However, mechanical energy supply was also not necessarily a good indicator of lateral oceanic heat transport in their models, with the former being dominated by wind variations in the Southern Ocean while the latter was dominated by wind variations in the tropics. Therefore care is required in interpreting our (and others) wind work tendencies in terms of changes in climate. In particular, our experiments have three noteworthy caveats when considering their application to the real ocean:

[43] 1. The use of relatively high vertical mixing rates might to some extent determine the magnitude of the response of the ACC to wind stress, however the qualitative results should be unaffected.

[44] 2. Surface geostrophic velocity may be affected by relaxing surface buoyancy flux boundary conditions, which might pin outcropping isopycnals to the same locations as in CNTRL, thus artificially constraining the path of the ACC and the latitude and extent of the Southern Hemisphere subtropical gyres. The same caveat was acknowledged by *Gnanadesikan and Hallberg* [2000] who found no major distinctions between their coarse-resolution model with a surface restoration scheme and preliminary integrations of a model coupled to an atmospheric energy balance model, with freely varying sea surface temperatures. Indeed, experiments with a range of different surface relaxation boundary conditions produce similar results when forced with N10DEG and S10DEG winds [*Lauderdale*, 2010]. The density field may also allow a certain degree of decoupling of the ACC from the topography, allowing it to cross geostrophic contours [e.g., *Borowski et al.*, 2002] instead of being steered by them. *Lu and Stammer* [2004] calculated the vorticity budget for two configurations of MITgcm similar to the one employed here. Their first model was initiated from climatology and was forced by relaxation to sea surface temperature and salinity fields whilst the second had no restoring but was forced by initial conditions and surface fluxes derived by data assimilation. They found that indeed, the abyssal density field was important in determining differences between the two deep ocean and vertically integrated flow fields. Although these models differed in the details of the dynamical balance, they still returned the same large scale distributions of Sverdrup flow, wind stress curl and bottom pressure torque, which compares well to higher resolution, eddy-permitting models [e.g., *Hughes and de Cuevas*, 2001] with different initial conditions and surface buoyancy fluxes.

[45] 3. Mesoscale eddies are known to play a central role in the response of the ACC to changes in wind forcing on time scales of years to decades [*Meredith and Hogg*, 2006; *Böning et al.*, 2008]. On these time scales, the ACC transport has been shown to be insensitive to changes in wind stress magnitude in eddying ocean models [*Hallberg and Gnanadesikan*, 2006; *Hogg et al.*, 2008; *Hutchinson et al.*, 2010], in clear contrast to coarse-resolution model results. On the other hand, it has been suggested that the timescale of adjustment of the density structure of the ACC and the global pycnocline in the eddying regime is long, of the order of centuries, therefore changes in ACC transport might not be detected in the current time series of Southern Ocean observations [*Jones et al.*, 2011; *Shakespeare and Hogg*, 2012]. This discrepancy between fast pycnocline adjustment in coarse resolution models and slow pycnocline adjustment in eddying models and possibly the real ocean might explain the greater values of wind work in S03STRONG in this study compared to the higher resolution model used by *Saenko et al.* [2005] and particularly observations of the ACC used by *Huang et al.* [2006]. The direct effect of mesoscale eddies on the rate of wind work is calculated to be small [*Scott*, 1999; *Scott and Xu*, 2009] even in regions of high eddy kinetic energy primarily due to the mismatch between the size of oceanic and atmospheric mesoscale features and particularly outside the equatorial regions, "eddy wind work" might be negative [*Hughes and Wilson*, 2008].

[46] Thus, our results regarding changes in wind work associated with wind-induced variations in the magnitude of ACC surface velocity should be considered for now in the context of an ocean model with parameterized eddies. In contrast, we expect our results concerning changes in wind work arising from variations in the spatial correlation between the westerlies and the ACC to hold in the eddying regime. This is because the dynamics underpinning the relative insensitivity of the ACC's large-scale pathway do not

depend critically on eddy processes. An illustration of this is provided by *Eden and Olbers* [2010], who show that the large-scale dynamical balance in two versions of a model of an ocean basin (one coarse-resolution, the other high-resolution) is unaffected by nonlinear (eddy) terms. *Hughes and de Cuevas* [2001] also demonstrate in their eddy-permitting model that nonlinear terms are unimportant for maintaining the broad features of the large-scale circulation. We therefore conclude that the sensitivity of wind work on the ocean's circulation to meridional shifts in the Southern Ocean winds highlighted by our study is likely a genuine feature of the climate system.

[47] **Acknowledgments.** Thanks to Anand Gnanadesikan, Andy Hogg, J. R. Toggweiler and Ric Williams for insightful comments that have greatly improved this work. JML was supported by a UK NERC PhD Studentship (NER/S/A/2006/14210) and UK NERC grant NE/G018782/1.

References

Adkins, J. F., K. McIntyre, and D. P. Schrag (2002), The salinity, temperature and $\delta^{18}O$ of the glacial deep ocean, *Science*, *298*, 1769–1773.

Allison, L., H. L. Johnson, D. Marshall, and D. R. Munday (2010), Where do winds drive the Antarctic Circumpolar Current?, *Geophys. Res. Lett.*, *37*, L12605, doi:10.1029/2010GL043355.

Anderson, R. F., S. Ali, L. I. Bradtmiller, S. H. H. Nielsen, M. Q. Fleisher, B. E. Anderson, and L. H. Burckle (2009), Wind-driven upwelling in the Southern Ocean and the deglacial rise in atmospheric CO_2, *Science*, *323*, 1443–1448, doi:10.1126/science.1167441.

Arbic, B. K., J. X. Mitrovica, D. R. MacAyeal, and G. A. Milne (2008), On the factors behind large labrador sea tides during the last glacial cycle and the potential implications for heinrich events, *Paleoceanography*, *23*, PA3211, doi:10.1029/2007PA001573.

Böning, C. W., A. Dispert, M. Visbeck, S. R. Rintoul, and F. U. Schwartzkopf (2008), The response of the Antarctic Circmpolar Current to recent climate change, *Nat. Geosci.*, *1*, 864–869, doi:10.1038/ngeo362.

Borowski, D., R. Gerdes, and D. Olbers (2002), Thermohaline and wind forcing of a circumpolar channel with blocked geostrophic contours, *J. Phys. Oceanogr.*, *32*, 2520–2540.

Butchart, N., et al. (2010), Chemistry–climate model simulations of twenty-first century stratospheric climate and circulation changes, *J. Clim.*, *23*(20), 5349–5374, doi:10.1175/2010JCLI3404.1.

Cai, W., and P. G. Baines (1996), Interactions between thermohaline- and wind-driven circulations and their relevance to the dynamics of the Antarctic Circumpolar Current, in a coarse-resolution global ocean general circulation model, *J. Geophys. Res.*, *101*(C6), 14,073–14,093.

Cunningham, S. A., S. G. Alderson, B. A. King, and M. A. Brandon (2003), Transport and variability of the Antarctic Circumpolar Current in Drake Passage, *J. Geophys. Res.*, *108*(C5), 8084, doi:10.1029/2001JC001147.

Dee, D. P., et al. (2011), The ERA-interim reanalysis: Configuration and performance of the data assimilation system, *Q. J. R. Meteorol. Soc.*, *137*(656), 553–597, doi:10.1002/qj.828.

Duhaut, T. H. A., and D. N. Straub (2006), Wind stress dependence on ocean surface velocity: Implications for mechanical energy input to ocean circulation, *J. Phys. Oceanogr.*, *36*(2), 202–211, doi:10.1175/JPO2842.1.

Eden, C., and D. Olbers (2010), Why western boundary currents are diffusive: A link between bottom pressure torque and bolus velocity, *Ocean Modell.*, *32*, 14–24, doi:10.1016/j.ocemod.2009.07.003.

Egbert, G. D., and R. D. Ray (2000), Significant dissipation of tidal energy in the deep ocean inferred from satilite altimeter data, *Nature*, *405*, 775–778.

Egbert, G. D., R. D. Ray, and B. G. Bills (2004), Numerical modelling of the global semidiurnal tide in the present day and the last glacial maximum, *J. Geophys. Res.*, *109*, C03003, doi:10.1029/2003JC001973.

Fyfe, J. C., and O. A. Saenko (2005), Human-induced changes in the Antarctic Circumpolar Current, *J. Clim.*, *18*, 3068–3073.

Ganachaud, A., and C. Wunsch (2000), Improved estimates of global ocean circulation, heat transport and mixing from hydrographic data, *Nature*, *408*, 453–457.

Gent, P. R., and J. McWilliams (1990), Isopycnal mixing in ocean circulation models, *J. Phys. Oceanogr.*, *20*, 150–155.

Gnanadesikan, A., and R. Hallberg (2000), On the relationship of the circumpolar current to Southern Hemisphere winds in coarse-resolution ocean models, *J. Phys. Oceanogr.*, *30*, 2013–2034.

Gnanadesikan, A., R. D. Slater, P. S. Swathi, and G. K. Vallis (2005), The energetics of ocean heat transport, *J. Clim.*, *18*(14), 2604–2616, doi:10.1175/JCLI3436.1.

Govin, A., E. Michel, L. D. Labeyrie, C. Waelbroeck, F. Dewilde, and E. Jansen (2009), Evidence for northward expansion of Antarctic Bottom Water in the Southern Ocean during the Last Glacial Maximum, *Paleoceanography*, *24*, PA1202, doi:10.1029/2008PA001603.

Green, J. A. M., C. L. Green, G. R. Bigg, T. P. Rippeth, J. D. Scourse, and K. Uehara (2009), Tidal mixing and the meridional overturning circulation from the Last Glacial Maximum, *Geophys. Res. Lett.*, *36*, L15603, doi:10.1029/2009GL039309.

Hallberg, R., and A. Gnanadesikan (2006), The role of eddies in determining the structure and response of the wind-driven Southern Hemisphere overturning: Results from the modeling eddies in the Southern Ocean (MESO) project, *J. Phys. Oceanogr.*, *36*, 2232–2252.

Hogg, A. M., M. P. Meredith, J. Blundell, and C. Wilson (2008), Eddy heat flux in the Southern Ocean: Response to variable wind forcing, *J. Clim.*, *21*, 608–620.

Huang, R. X., W. Wang, and L. L. Liu (2006), Decadal variability of wind-energy input to the world ocean, *Deep Sea Res., Part II*, *53*(1–2), 31–41, doi:10.1016/j.dsr2.2005.11.001.

Hughes, C. W., and B. de Cuevas (2001), Why western boundary currents in realistic oceans are inviscid: A link between form stress and bottom pressure torques, *J. Phys. Oceanogr.*, *31*, 2871–2885.

Hughes, C. W., and C. Wilson (2008), Wind work on the geostrophic circulation: An observational study of the effect of small scales in the wind stress, *J. Geophys. Res.*, *113*, C02016, doi:10.1029/2007JC004371.

Hutchinson, D. K., A. M. C. Hogg, and J. R. Blundell (2010), Southern Ocean response to relative velocity wind stress forcing, *J. Phys. Oceanogr.*, *40*(2), 326–339, doi:10.1175/2009JPO4240.1.

Jackson, L., C. W. Hughes, and R. G. Williams (2006), Topographic control of basin and channel flows: The role of bottom pressure torques and friction, *J. Phys. Oceanogr.*, *36*, 1786–1805.

Jiang, S., P. H. Stone, and P. Malanotte-Rizzoli (1999), An assessment of the Geophysical Fluid Dynamics Laboratory ocean model with coarse resolution: Annual-mean climatology, *J. Geophys. Res.*, *104*, 25,623–25,645.

Jones, D. C., T. Ito, and N. S. Lovenduski (2011), The transient response of the Southern Ocean pycnocline to changing atmospheric winds, *Geophys. Res. Lett.*, *38*, L15604, doi:10.1029/2011GL048145.

Kitoh, A., S. Murakami, and H. Koide (2001), A simulation of the Last Glacial Maximum with a coupled atmosphere-ocean GCM, *Geophys. Res. Lett.*, *28*, 2221–2224, doi:10.1029/2000GL012271.

Lauderdale, J. M. (2010), On the role of the Southern Ocean in the global carbon cycle and atmospheric CO_2 change, PhD thesis, Sch. of Ocean and Earth Sci., Univ. of Southampton, Southampton, U. K.

Lu, Y., and D. Stammer (2004), Vorticity balance in coarse-resolution global ocean simulations, *J. Phys. Oceanogr.*, *34*(3), 605–622, doi:10.1175/2504.1.

Luyten, J. R., J. Pedlosky, and H. Stommel (1983), The ventilated thermocline, *J. Phys. Oceanogr.*, *13*(2), 292–309, doi:10.1175/1520-0485(1983)013<0292:TVT>2.0.CO;2.

Marshall, J., A. Adcroft, C. Hill, L. Perelman, and C. Heisey (1997), A finite-volume, incompressible Navier Stokes model for studies of the ocean on parallel computers, *J. Geophys. Res.*, *102*(C3), 5753–5766.

Matsumoto, K., J. Lynch-Stieglitz, and R. F. Anderson (2001), Similar glacial and Holocene Southern Ocean hydrography, *Paleoceanography*, *16*(5), 445–454.

Maximenko, N., P. Niiler, L. Centurioni, M.-H. Rio, O. Melnichenko, D. Chambers, V. Zlotnicki, and B. Galperin (2009), Mean dynamic topography of the ocean derived from satellite and drifting buoy data using three different techniques, *J. Atmos. Oceanic Technol.*, *26*(9), 1910–1919, doi:10.1175/2009JTECHO672.1.

Menviel, L., A. Timmerman, A. Mouchet, and O. Timm (2008), Climate and marine carbon response to changes in the strength of the Southern Hemispheric westerlies, *Paleoceanography*, *33*, PA4201, doi:10.1029/2008PA001604.

Meredith, M. P., and A. M. Hogg (2006), Circumpolar response of Southern Ocean eddy activity to a change in the Southern Annular Mode, *Geophys. Res. Lett.*, *35*, L16608, doi:10.1029/2006GL026499.

Munk, W. H., and E. Palmén (1951), Note on the dynamics of the Antarctic Circumpolar Current, *Tellus*, *3*, 472–474.

Munk, W. H., and C. Wunsch (1998), Abyssal recipes II: Energetics of tidal and wind mixing, *Deep-Sea Res., Part I*, *45*, 1977–2010.

Nikurashin, M., and R. Ferrari (2011), Global energy conversion rate from the geostrophic flows into internal lee waves in the deep ocean, *Geophys. Res. Lett.*, *38*, L08610, doi:10.1029/2011GL046576.

Oke, P. R., and M. H. England (2004), Oceanic response to changes in the latitude of the Southern Hemisphere subpolar westerly winds, *J. Clim.*,

17(5), 1040–1054, doi:10.1175/1520-0442(2004)017<1040:ORTCIT>2.0.CO;2.

Olbers, D., D. Borowski, C. Völker, and J.-A. Wölff (2004), The dynamical balance, transport and circulation of the Antarctic Circumpolar Current, *Antarct. Sci.*, *16*(4), 439–470, doi:10.1017/S0954102004002251.

Oliver, K. I. C., and N. R. Edwards (2008), Location of potential energy sources and the export of dense water from the Atlantic Ocean, *Geophys. Res. Lett.*, *35*, L22604, doi:10.1029/2008GL035537.

Otto-Bliesner, B., E. C. Brady, G. Clauzet, R. Tomas, S. Levis, and Z. Kothavala (2006), Last Glacial Maximum and Holocene climate in CCSM3, *J. Clim.*, *19*, 2526–2544.

Perlwitz, J., S. Pawson, R. L. Fogt, J. E. Nielsen, and W. D. Neff (2008), Impact of stratospheric ozone hole recovery on Antarctic climate, *Geophys. Res. Lett.*, *35*, L08714, doi:10.1029/2008GL033317.

Polvani, L. M., M. Previdi, and C. Deser (2011), Large cancellation, due to ozone recovery, of future Southern Hemisphere atmospheric circulation trends, *Geophys. Res. Lett.*, *38*, L04707, doi:10.1029/2011GL046712.

Russell, J. L., R. J. Stouffer, and K. W. Dixon (2006a), Intercomparison of the Southern Ocean circulations in IPCC coupled model control simulations, *J. Clim.*, *19*(18), 4560–4575, doi:10.1175/JCLI3869.1.

Russell, J. L., K. W. Dixon, A. Gnanadesikan, R. J. Stouffer, and J. R. Toggweiler (2006b), The Southern Hemisphere westerlies in a warming world: Propping open the door to the deep ocean, *J. Clim.*, *19*, 6382–6390.

Saenko, O. A., J. C. Fyfe, and M. H. England (2005), On the response of the oceanic wind-driven circulation to atmospheric CO_2 increase, *Clim. Dynam.*, *25*, 415–426.

Scott, R. B. (1999), Geostrophic energetics and the small viscosity behaviour of an idealized ocean circulation model, PhD thesis, McGill Univ., Montreal, Que., Canada.

Scott, R. B., and Y. Xu (2009), An update on the wind power input into the surface geostrophic flow of the world ocean, *Deep Sea Res., Part I*, *56*, 295–304, doi:10.1016/j.dsr.2008.09.010.

Scott, R. B., J. A. Goff, A. C. Naveira Garabato, and A. J. G. Nurser (2011), Global rate and spectral characteristics of internal gravity wave generation by geostrophic flow over topography, *J. Geophys. Res.*, *116*, C09029, doi:10.1029/2011JC007005.

Sen Gupta, A., and M. H. England (2006), Coupled ocean-atmosphere-ice response to variations in the southern annular mode, *J. Clim.*, *19*(18), 4457–4486, doi:10.1175/JCLI3843.1.

Shakespeare, C. J., and A. M. Hogg (2012), An analytical model of the response of the meridional overturning circulation to changes in wind and buoyancy forcing, *J. Phys. Oceanogr.*, doi:10.1175/JPO-D-11-0198.1, in press.

Shin, S. I., Z. Liu, B. Otto-Bliesner, E. C. Brady, J. E. Kutzbach, and S. P. Harrison (2003), A simulation of the Last Glacial Maximum climate using the NCAR-CCSM, *Clim. Dyn.*, *20*, 127–151.

Shulmeister, J., et al. (2004), The Southern Hemisphere westerlies in the Australasian sector over the last glacial cycle: A synthesis, *Quat. Int.*, *118–119*, 23–53, doi:10.1016/S1040-6182(03)00129-0.

Thompson, D. W. J., and S. Solomon (2002), Interpretation of recent Southern Hemisphere climate change, *Science*, *296*, 895–899, doi:10.1126/science.1069270.

Toggweiler, J. R., and B. L. Samuels (1998), On the ocean's large-scale circulation near the limit of no vertical mixing, *J. Phys. Oceanogr.*, *28*, 1832–1852.

Toggweiler, J. R., J. L. Russell, and S. R. Carson (2006), Midlatitude westerlies, atmospheric CO_2 and climate change during the ice ages, *Paleoceanography*, *21*, PA2005, doi:10.1029/2005PA001154.

Trenberth, K., J. Olson, and W. Large (1989), A global wind stress climatology based on ECMWF analyses, *Tech. Rep. NCAR/TN-338+STR*, Natl. Cent. for Atmos. Res., Boulder, Colo.

Tschumi, T., F. Joos, and P. Parekh (2008), How important are the Southern Hemisphere wind changes for low glacial carbon dioxide?, *Paleoceanography*, *34*, PA4208, doi:10.1029/2008PA001592.

Watson, A. J., and A. C. Naveira Garabato (2006), The role of Southern Ocean mixing and upwelling in glacial-interglacial atmospheric CO_2 change, *Tellus B*, *58*, 73–87.

Webb, D. J., and N. Suginohara (2001), Oceanography: Vertical mixing in the ocean, *Nature*, *409*(6816), 37–37.

Williams, G. P., and K. Bryan (2006), Ice age winds: An aquaplanet model, *J. Clim.*, *19*, 1709–1715.

Wunsch, C. (1998), The work done by the wind on the oceanic general circulation, *J. Phys. Oceanogr.*, *28*, 2332–2340.

Yang, X.-Y., R. X. Huang, and D. X. Wang (2007), Decadal changes of wind stress over the Southern Ocean associated with Antarctic ozone depletion, *J. Clim.*, *20*(14), 3395–3410, doi:10.1175/JCLI4195.1.